IL NUOVO CIMENTO **47 C** (2024) 75
DOI 10.1393/ncc/i2024-24075-2

Colloquia: IFAE 2023

Search for CP violation in the interactions of the Higgs boson with vector bosons with the ATLAS experiment(*)

C. Arcangeletti on behalf of the ATLAS Collaboration
INFN Laboratori Nazionali di Frascati - Frascati, Italy

received 13 February 2024

Summary. — One of the primary research objectives at CERN's Large Hadron Collider (LHC) is to comprehensively understand the Higgs boson and how it interacts with other particles. Advanced analysis methods are used to extract the best information from data on how the Higgs boson couples with fundamental particles. Several investigations aimed at exploring any unusual effects in the way the Higgs boson interacts with vector bosons and its charge-parity properties are presented. These studies are conducted using a dataset of 139 fb^{-1} gathered by the ATLAS experiment through proton-proton collisions at a center-of-mass energy of 13 TeV.

1. – Introduction

The asymmetry between the matter and antimatter content in the Universe is one of the unsolved problems in physics. This implies the violation of charge conjugation and parity symmetry (CP). The Standard Model (SM) can only account for a small portion of the CP violation required. Therefore, other sources of CP violation must exist Beyond the Standard Model (BSM). In the Standard Model, the Higgs boson is a CP-even scalar particle with $J^{CP} = 0^{++}$. Any sign of CP violation would imply BSM Physics. During LHC Run 1 ($\sqrt{s}$ = 7-8 TeV, 25 fb^{-1}), the ATLAS experiment [1] aimed to demonstrate that the Higgs boson is CP-even. Tests with fixed hypotheses of spin and parity $J^P = 0^+$ were compared to alternative spin models. Non-SM hypotheses were excluded at 99.9% confidence level (CL) in favor of a Higgs boson with Spin/Parity 0^{++} [2]. Identification of CP-even and CP-odd states was achieved by examining the tensor structure of the HVV interaction, namely the Higgs boson interaction with two vector bosons, which showed excellent agreement with the Standard Model. This approach was also followed during LHC Run 2 ($\sqrt{s}$ = 13 TeV, 139 fb^{-1}), studying other Higgs interaction vertices, not only its decays but also its production processes.

2. – Study the CP structure of the HVV interaction vertex

CP violation effects in the interaction between the Higgs boson and vector bosons can be investigated through two fundamental processes: production via vector boson fusion

(*) IFAE 2023 - "Energy Frontier" session

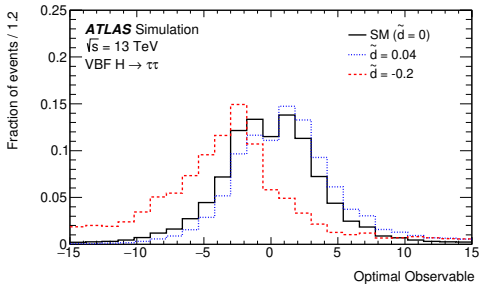

Fig. 1. – Distribution of the Optimal Observable for signal events for three example values of $\tilde{d}$. Non-vanishing values of $\tilde{d}$ cause an asymmetry and a non-vanishing mean value [8].

(VBF) and decay into two Z bosons ($H \to ZZ^* \to 4\ell$). The ATLAS Collaboration published few results regarding these processes. The production through VBF has been studied in the decay channels $H \to \tau\tau$ (36.1 fb^{-1}) [8], $H \to \gamma\gamma$ (139 fb^{-1}) [9], and $H \to ZZ^* \to 4\ell$ (139 fb^{-1}), which also examined the decay vertex. Those analyses are based solely on the shape of observable distributions sensitive to CP effects. They ignore the dependence of the cross-section on possible CP-mixing scenarios. Limits are set on CP-odd couplings based on Effective Field Theory models.

Information about the particle kinematics resulting from various processes can be sensitive to CP effects. To maximise the sensitivity, they can be combined into a single highly sensitive variable: the *Optimal Observable* (OO) [3-5]. It is a Matrix Element based variable, comprising both a CP-even SM contribution and a CP-odd BSM contribution of the Higgs boson interaction. In the amplitude is then possible to distinguish two terms: an interference term sensitive only to CP-odd effects and a quadratic BSM term sensitive only to the coupling strength. The interference is symmetric for SM-like contributions and asymmetric for CP-odd contributions, as shown in fig. 1, making it sensitive to the sign of the coupling. For this reason the Optimal Observables used in this searches are expressed as the ratio of the interference term and quadratic SM element:

$$\mathcal{OO} = \frac{2\Re\left(\mathcal{M}^*_{\mathrm{SM}}\mathcal{M}_{\mathrm{BSM}}\right)}{\left|\mathcal{M}_{\mathrm{SM}}\right|^2}. \tag{1}$$

Beyond the Standard Model effects are parameterized as perturbative terms of higher orders in the Standard Model Lagrangian (valid up to an energy scale $\Lambda \sim 1$ TeV)

$$\mathcal{L}_{\mathrm{SMEFT}} = \mathcal{L}_{\mathrm{SM}} + \sum_i \frac{c_i}{\Lambda^2} O_i^{(6)} \ , \tag{2}$$

in what is known as Standard Model Effective Field Theory (SMEFT) [6]. A complete set of dimension-6 operators includes three independent CP-odd couplings, and different bases can be defined according to the assumptions made. In the analyses that will be discussed results have been presented in three bases. The *Warsaw Basis* consists in the eigenvectors of fields before symmetry breaking and the couplings are expressed as $c_{H\tilde{W}}$, $c_{H\tilde{B}}$ and $c_{H\tilde{W}B}$. With these operators it is possible to build another basis [7] that can probe the effects of the Higgs boson couplings to other particles, and is more closely linked to experimental physical observables than the Warsaw basis. It is called *Higgs basis* and

it consists instead on mass eigenstates after symmetry breaking and the couplings are expressed as $\tilde{c}_{zz}$, $\tilde{c}_{z\gamma}$ and $\tilde{c}_{\gamma\gamma}$. Finally, the *Hawk Basis* assumes that the BSM CP-odd Higgs boson coupling to a $Z\gamma$ pair is zero and that the two remaining CP-odd couplings in the Warsaw basis, which mix to form the two couplings of the Higgs boson to ZZ^* and $\gamma\gamma$ decays, are the same. The single remaining effective coupling is denoted by $\tilde{d}$.

3. – CP violation in the VBF production in $H \to \tau\tau$ [8] and $H \to \gamma\gamma$ [9] decay channels

In the $H \to \tau\tau$ analysis, selected events were categorized as di-leptonic with the same flavor (τlepτlep SF), di-leptonic with different flavors (τlepτlep DF), semi-leptonic (τlepτhad SF), or fully hadronic (τhadτhad). For $H \to \gamma\gamma$, events were chosen based on the presence of two photons with a mass falling within the range of 105 GeV to 160 GeV. To identify VBF signals, criteria were applied for both $H \to \tau\tau$ and $H \to \gamma\gamma$. For $H \to \tau\tau$, this included the presence of at least two jets ($N_{jets} \geq 2$) and the application of a Boosted Decision Tree (BDT) to differentiate the VBF signal from the background. A cut on the BDT score was used to define the signal region (SR). Control regions (CR) were also established to constrain background contributions. In the case of $H \to \gamma\gamma$, selection criteria encompassed the presence of at least two jets ($N_{jets} \geq 2$), a significant separation in pseudorapidity between the two leading jets ($\Delta\eta_j j > 2$), and the value of $\eta^{Zepp} = \eta_{\gamma\gamma} - (\eta_{j1} + \eta_{j2})/2$ falling below 5. Two BDTs were applied to distinguish between VBF and ggF (gluon-gluon fusion) production modes and VBF and continuous background. Cuts on these BDT scores were employed to define three distinct signal regions. To measure couplings, optimal observables were constructed based on the kinematic information of the Higgs plus 2-jet system . For $H \to \tau\tau$, a simultaneous maximum likelihood fit was performed, using both the distribution of optimal observables in the SR and the invariant mass of the $\tau\tau$ system in the CR. For $H \to \gamma\gamma$, a simultaneous maximum likelihood fit was applied to the distribution of the invariant mass of the two photons in each optimal observable bin, within every signal region. The observed limits for the coupling $\tilde{d}$ were set. For $H \to \tau\tau$, the coupling range was determined as [-0.090, 0.300] at 68% CL [8]. For $H \to \gamma\gamma$, the coupling range was established as [-0.010, 0.040] at 68% CL [9]. In the combined analysis of both processes, the coupling range was found to be [-0.012, 0.030] at 68% CL (fig. 2) [9].

4. – CP violation in the VBF production and in the $H \to ZZ^* \to 4\ell$ decay channel [10]

During the event selection for the $H \to ZZ^* \to 4\ell$ process, events were categorized based on specific criteria. This included identifying two pairs of same-flavor but opposite-charge leptons, each having transverse momenta (p_T) exceeding 20, 15, 10, and 5 GeV while ensuring they were well-isolated. Invariant mass conditions were applied, requiring $50 < m_{12} < 106$ GeV for the leading pair and $m_{thr} < m_{34} < 115$ GeV for the sub-leading one (where m_{thr}=12 GeV if m_{4l} <140 GeV and rises linearly until reaching 50 GeV for m_{4l}=190 GeV), with an additional constraint that the invariant mass m_{4l} fell within the range of 105 GeV to 160 GeV, defining what is known as the Inclusive Signal Region (Inclusive SR). To identify the VBF signal, a set of criteria was applied, requiring events to have at least two jets ($N_{jets} \geq 2$), an invariant mass of jet pairs (m_{jj}) greater than 120 GeV, and the invariant mass of the four leptons (m_{4l}) falling within the range of 115 to 130 GeV. A neural network (NN) was employed to discriminate between VBF,

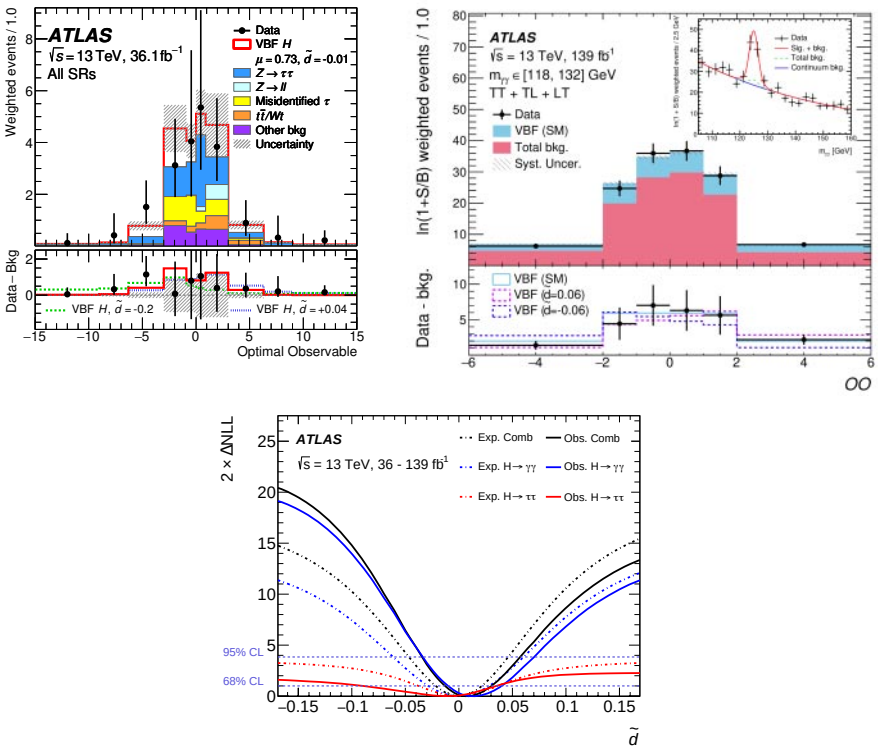

Fig. 2. – (Top-left) Distribution of the OO for all four SRs combined in the $H \to \tau\tau$ analysis [8]. (Top-right) Distribution of the OO summing together the contribution of all the SRs in the $H \to \gamma\gamma$ analysis [9]. (Bottom) Comparison of the ΔNLL curves as function of $\tilde{d}$ for the $H \to \tau\tau$, $H \to \gamma\gamma$ analysis and their combination [9].

VH, and ggF signals, effectively defining four different signal regions (VBF SR 1-4). The analysis considered several main backgrounds. For non-resonant ZZ^* production, the normalization was constrained in control regions (ZZ* CR), specifically for m_{4l} ranges of [105-115] GeV and [130-160] GeV. For reducible backgrounds such as $Z + jets$, $t\bar{t}$, WZ, estimations were made using data and different control regions, with separate estimations for processes involving $\ell\ell\mu\mu$ and $\ell\ell ee$. Backgrounds such as tXX (as $t\bar{t}Z$, $t\bar{t}W$, tWZ) and tri- vector bosons production VVV were determined through Monte Carlo simulations. In the case of VBF production, contributions from the ggF process were also considered as a background, with their impact constrained in a control region known as the VBF-depleted Region, which was orthogonal to the VBF selection.

The measurement of couplings involved various analysis levels, contingent on the specific process under investigation. At the production level, the analysis had sensitivity to CP-odd effects in both the VBF production vertex and the $H \to ZZ^*$ decay vertex. Distributions of Optimal Observables for the Higgs plus 2-jet system (OO_{jj}) were constructed and simultaneously fitted in the four VBF signal regions (VBF SR 1-4). The normalization of ZZ^* and ggF backgrounds was incorporated into the fit in their respective control regions (CR). At the decay level, CP-odd effects were exclusively studied at the $H \to ZZ^*$ decay vertex. Distributions of Optimal Observables for the Higgs in four

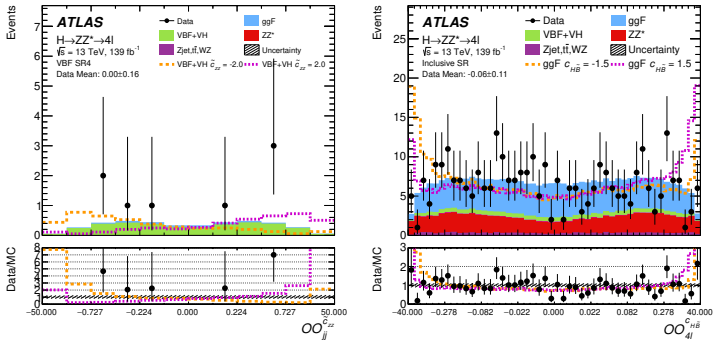

Fig. 3. – The observed and expected distributions for the production-level $OO^{\tilde{c}_{zz}}_{1,jj}$ in the VBF region SR4 (on the left) and for the decay-level $OO^{c_{H\tilde{B}}}_{1,4l}$ in the inclusive SR (on the right) [10].

leptons ($OO_{4\ell}$) were constructed and fitted in the inclusive signal region. The normalization of the ZZ^* background was constrained within the ZZ^* CR. Lastly, a combination approach involved a simultaneous fit for OO_{jj} in the VBF regions and $OO_{4\ell}$ in the depleted region.

The reported results were not uniform across all analysis approaches, as not all approaches were equally sensitive to all couplings. Consequently, the best limits obtained from individual approaches were highlighted. Overall, these results were consistent with the expectations outlined by the Standard Model. In a general sense, limits obtained from decay events were notably more stringent due to their superior statistical significance, with approximately 200 events compared to only around 10 VBF events. The limits on sensitive EFT coupling are summarized in fig. 4.

Unfolded measurements of the Optimal Observables were provided in this analysis [10]. A measurement of the distribution of differential cross-sections of OO offers the possibility of a measurement that is more independent of models than those previously illustrated. This allows for the reinterpretation of results in various models that predict CP violation. The measurement of differential cross-sections in the fiducial region for the $H \to ZZ^* \to 4\ell$ channel starts from the definition of a fiducial volume based on the detector's acceptance to minimize model-dependent dependencies. Then to correct for detector resolution effects and accounting for migrations through the use of an unfolding process based on the detector response matrix is performed. Finally the signal extraction is carried out by fitting the distribution of m_{4l} in each bin of the optimal observables distribution.

5. – Conclusions

The study of the Spin/Parity properties of the Higgs boson constitutes an important field for probing physics beyond the Standard Model. Investigating signs of CP violation in Higgs couplings has been a key focus of research. Studies conducted with the ATLAS experiment at LHC using data collected at 13 TeV have explored Higgs couplings with vector bosons in VBF production as well as at the decay vertex in the $H \to ZZ^* \to 4\ell$ channel. Various theoretical approaches within the framework of Effective Field Theory (EFT) have been employed to investigate different couplings. Optimal Observables were utilized as variables, sensitive to the effects of CP-odd couplings. In the $H \to ZZ^* \to 4\ell$,

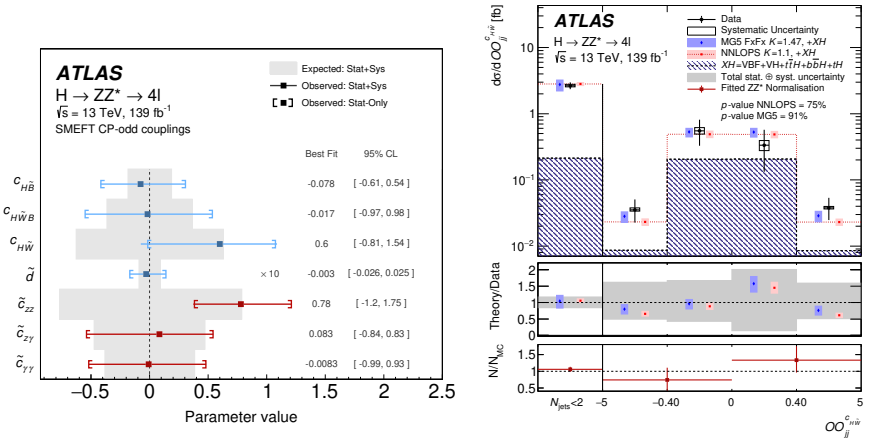

Fig. 4. – (On the left) The expected and observed measurements of the CP-odd Wilson coefficients [10]. (On the right) Differential fiducial cross-section for the optimal observables $OO^{c_{H\tilde{W}}}_{1,jj}$ [10].

measurements of the fiducial differential cross-sections of these observables were provided, allowing for potential reinterpretation. Thus far, no evidence of CP violation effects has been observed. These findings constitute an important step in our understanding of the Higgs boson's behavior.

REFERENCES

[1] ATLAS Collaboration, *JINST*, **3** (2008) S08003.
[2] ATLAS Collaboration, *Eur. Phys. J. C*, **75** (2015) 476; **76** (2016) 152(E).
[3] Atwood D. and Soni A., *Phys. Rev. D*, **45** (1992) 2405.
[4] Davier M., Duflot L., Le Diberder F. and Rouge A., *Phys. Lett. B*, **306** (1993) 411.
[5] Diehl M. and Nachtmann O., *Optimal observables for measuring three-gauge-boson couplings in* $e^+e^- \to W^+W^-$, arXiv:hep-ph/9603207.
[6] Brivio I. and Trott M., *Phys. Rep.*, **793** (2019) 1.
[7] LHC Higgs Cross Section Working Group (de Florian D. *et al.*), *Handbook of LHC Higgs Cross Sections: 4. Deciphering the Nature of the Higgs Sector.*
[8] ATLAS Collaboration, *Phys. Lett. B*, **805** (2020) 135426.
[9] ATLAS Collaboration, *Phys. Rev. Lett.*, **131** (2023) 061802.
[10] ATLAS Collaboration, *Test of CP-invariance of the Higgs boson in vector-boson fusion production and its decay into four leptons*, arXiv:2304.09612 [hep-ex].